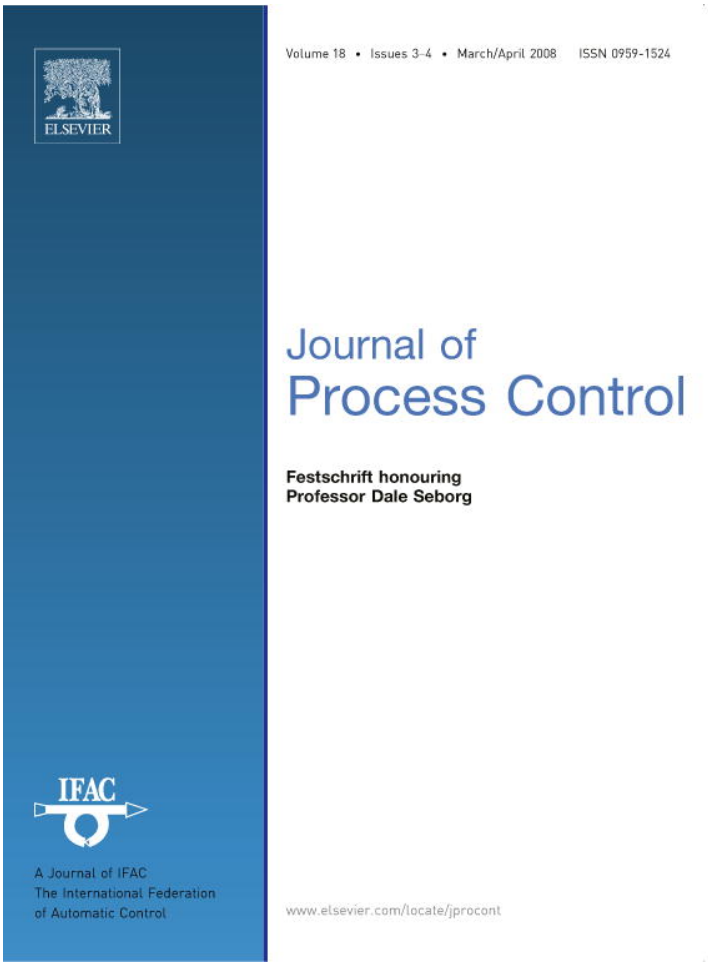

Available online at www.sciencedirect.com
ScienceDirect
Journal of Process Control 18 (2008) 399–407
JOURNAL OF PROCESS CONTROL
www.elsevier.com/locate/jprocont

Comparative performance of concentration and temperature controlled batch crystallizations

Zoltan K. Nagy [a], Jia W. Chew [b], Mitsuko Fujiwara [b], Richard D. Braatz [b,*]

[a] Chemical Engineering Department, Loughborough University, Loughborough LE11 3TU, United Kingdom
[b] Department of Chemical and Biomolecular Engineering, University of Illinois at Urbana-Champaign, 600 South Mathews Avenue, 93 Roger Adams Lab, Box C-3, Urbana, IL 61801, USA

Received 11 August 2007; accepted 3 October 2007

Abstract

An increased interest has been directed towards the crystallization of pharmaceuticals and proteins in recent years, which have additional complications compared to the extensively studied inorganic batch and continuous crystallizations. Recent advances in process analytical technology have enabled the improved modeling and control of batch crystallization. This paper compares simulations and experiments between the classical temperature control approach developed in the 1970–1990s with the concentration-control approach developed more recently. The latter approach, which uses attenuated total reflection–Fourier transform infrared (ATR–FTIR) spectroscopy and feedback control to follow a setpoint trajectory in the solution concentration as a function of temperature, results in reduced sensitivity of the product quality to certain disturbances. The resulting guidelines from the simulations are applied to the experimental investigation of the crystallization of paracetamol in water.

Keywords: Optimal control; Particulate processes; Parameter estimations

1. Introduction

Despite the long history and widespread application of batch crystallization, there are a disproportionate number of problems associated with its control. These problems have become especially important in recent years as an increased interest has been directed towards the crystallization of pharmaceuticals and proteins, which have additional complications compared to the inorganic batch and continuous crystallizations studied extensively over the past 50+ years. These complications include limited availability of the pharmaceutical, unexpected polymorphic phase transformation, and complex shape of organic crystals. Many problems in downstream processes can be attributed to poor particle characteristics established in the crystallization step. The control objectives for batch crystallization processes can be defined in terms of product purity, crystal habit, morphology, average particle size, crystal size distribution, bulk density, product filterability, and dry solid flow properties. Recent advances in sensor technology have brought on-line feedback control within the realm of possibility [1,2]. On-line control during batch crystallization offers the possibilities for improved crystal product quality, shorter process times, and reduction or elimination of compromised batches.

The fundamental driving force for crystallization from solution is the difference in the chemical potential between the solution and the solid phase; however, it is more convenient to write the driving force in terms of the supersaturation, which is the difference between the solution concentration and the saturation concentration. The size, shape, and solid-state phase of the product crystals are dependent on the supersaturation profile achieved during the crystallization process. Supersaturation is usually created by cooling, evaporation, or antisolvent addition. For

* Corresponding author. Tel.: +1 217 333 5073; fax: +1 217 333 5052.
E-mail address: braatz@uiuc.edu (R.D. Braatz).

0959-1524/$ - see front matter © 2007 Elsevier Ltd. All rights reserved.
doi:10.1016/j.jprocont.2007.10.006

brevity, this paper will primarily discuss cooling crystallization, although the principles apply to other methods of supersaturation creation.

Most past studies in batch crystallization control have dealt with finding the open-loop temperature versus time trajectory that optimizes some characteristics of the desired crystal size distribution, as discussed in several review papers [1,3]. This classical approach requires the development of a first-principles model with accurate growth and nucleation kinetics, which can be obtained in a series of continuous or batch experiments. Uncertainties in the parameter estimates, nonidealities in the model assumptions, and disturbances have to be taken into account to ensure that this approach results in the expected optimized product quality [4–8].

An alternative *direct design* approach to controlling a batch crystallizer is based on the understanding that the desired region of operation for most crystallizers is within the metastable zone (see Fig. 1), which is bounded by the solubility curve and the metastable limit [9]. This approach uses a feedback control system to follow a solution concentration trajectory as a function of temperature [10–13], where this setpoint trajectory is designed to lie within the metastable zone. The setpoint supersaturation curve is the result of the compromise between the desire for a fast crystal growth rate that occurs near the metastable limit, and a low nucleation rate, which takes place near the solubility curve. The advantage of this approach is that, unlike the first approach, it does not require the derivation of accurate growth and nucleation kinetics. It can be implemented with the knowledge of the solubility curve and an in situ concentration measurement. Increased interest in this approach is motivated by recent developments in in situ sensor technology, which allows automated determination of the solubility curve and the metastable limit [11,14].

This paper uses a combination of simulations and experiments to describe and compare the classical temperature control approach with the direct design approach. This assessment considers the effects of parameter uncertainties and disturbances for the crystallization of an important pharmaceutical, paracetamol (acetaminophen). A variety of disturbance scenarios (e.g., shifts in the solubility curve, deviations in seeding, evaporation) are investigated. The advantages and disadvantages of each control approach are discussed. Understanding these tradeoffs provide guidance as to the best control strategy for a particular crystallization process.

2. Batch system and operation

Usually the main objective of batch crystallization is to produce large uniform crystals within a given time. Since a large number of nuclei form if the supersaturation crosses the metastable limit, most crystallizers are operated by adding seeds near the start of the batch and maintaining the supersaturation within the metastable zone, where the nucleation and growth processes compete for the solute molecules. Both the nucleation and growth rates are positive monotonic functions of the supersaturation. An optimal control strategy should have a high enough supersaturation that the growth rate is significant (so that the batch runs are not too long) but low enough supersaturation to keep the rate of nucleation low. Seeding reduces the productivity of each batch somewhat, but can lead to more consistent product crystals. Seeds can be added or generated at the beginning of the batch. Fig. 2 shows typical operating lines for each method, in the concentration versus temperature diagram. For "seeded operation" the seed is introduced shortly after the solubility curve is crossed and the operating line should remain within the metastable zone. For "unseeded operation" where the seeds are generated in the batch, the operating line first reaches the metastable limit to generate seeds and then the supersaturation should be kept below the metastable limit similar to the seeded system.

Parameter estimation and control experiments were performed with paracetamol (4-acetamidophenol, 98%,

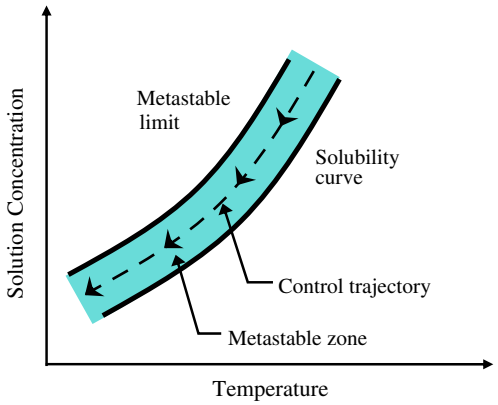

Fig. 1. The metastable zone, solubility curve, metastable limit, and concentration–temperature control trajectory. Similar notions apply to antisolvent and evaporative crystallization.

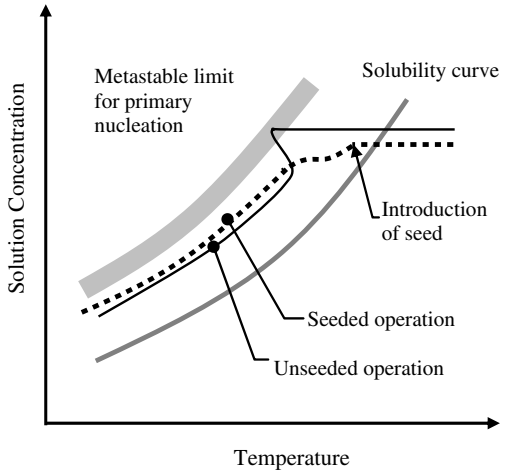

Fig. 2. Operations of seeded and unseeded batch cooling crystallizers.

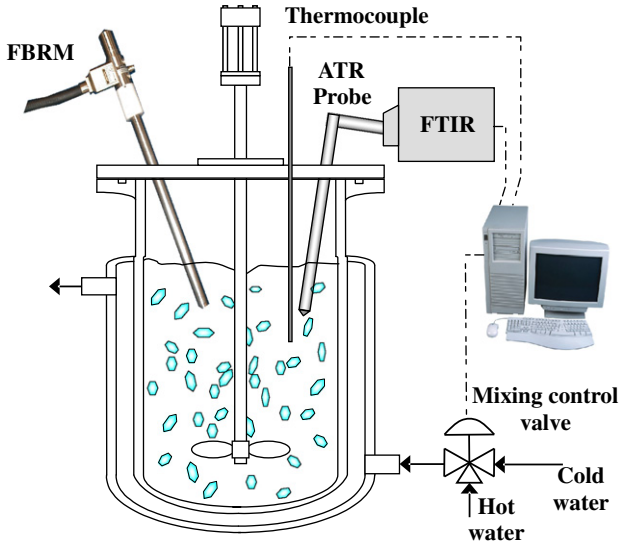

Fig. 3. Schematic representation of the experimental setup.

Aldrich) and degassed, deionized water in a 500 ml jacketed round bottom flask fitted with an overhead stirrer (see Fig. 3). During the experiments the solution concentration was measured using attenuated total reflection–Fourier transform infrared (ATR–FTIR) spectroscopy coupled with robust chemometrics as described previously [11,15]. Chord length distributions of paracetamol crystals in solution were obtained using Lasentec focused beam reflectance measurement (FBRM) connected to a Pentium III running version 6.0b9 of the FBRM control interface software. Geometric inverse modeling [16] was used to compute the particle size distribution from the chord length distribution, assuming spherical shapes and linear distribution in each bin. Although this assumption can lead to biased estimation of the crystal size distribution, it is a common assumption made in the literature, whenever kinetic parameters are estimated from PSD sensors that report spherical-equivalent diameters. The sample temperature was controlled based on thermocouple measurement by ratioing the hot and cold water to the jacket with a research control valve (Badger Meter, Inc.) using a proportional–integral control system designed via internal model control. To track the concentration–temperature trajectory, the same control system was used to manipulate the crystallizer jacket water flow based on solution concentration measurement as described previously [11]. The same instrument conditions were used for all experiments. Reagent grade acetanilide was obtained from Fisher.

3. Modeling and parameter estimation

This section describes how parameters are estimated in batch crystallization. Because the most popular parameter estimation algorithms iteratively call the simulation model, the method of moments is usually used to reduce the simulation time. The jth moment when there is one characteristic size dimension is

$$\mu_j = \int_0^\infty L^j f(L,t)\mathrm{d}L, \tag{1}$$

where $f(L,t)$ is the crystal size distribution, L is the crystal size, and t is time. Typically the four lowest order moments are simulated since many properties of the crystal size distribution (CSD) can be expressed as a function of these moments. After some simplifying assumptions [17], the model equations are:

$$\begin{aligned}
\frac{\mathrm{d}\mu_0}{\mathrm{d}t} &= B,\\
\frac{\mathrm{d}\mu_1}{\mathrm{d}t} &= G\mu_0 + Br_0,\\
\frac{\mathrm{d}\mu_2}{\mathrm{d}t} &= 2G\mu_1 + Br_0^2,\\
\frac{\mathrm{d}\mu_3}{\mathrm{d}t} &= 3G\mu_2 + Br_0^3,\\
\frac{\mathrm{d}C}{\mathrm{d}t} &= -\rho_c k_v(3G\mu_2 + Br_0^3)
\end{aligned} \tag{2}$$

where C is the solution concentration expressed in mass of crystal per unit mass of solvent, r_0 is the crystal size at nucleation, ρ_c is the density of the crystal, k_v is the volumetric shape factor, and B and G are the nucleation and growth rates, respectively. The growth kinetics are typically assumed to satisfy

$$G = k_g \Delta C^g, \tag{3}$$

with $\Delta C = C - C^*$ being the supersaturation. The solubility (C^*) is a function of temperature (T). For the paracetamol crystals used here as a demonstrative system, the experimentally determined solubility curve (with T in K) is [11]

$$C^*(T) = 1.5846 \times 10^{-5}T^2 - 9.0567 \times 10^{-3}T + 1.3066. \tag{4}$$

For the modeling performed here, the crystallizer is unseeded, which presents a more challenging control problem than the seeded case most commonly studied. Then the unseeded nucleation rate is given by

$$B = k_b \Delta C^b, \tag{5}$$

which is referred to as "primary nucleation" in the literature [9]. The initial condition for (2) is given by $\mu_i(0) = 0$ $(i = 0,1,2,3)$, and $C(0) = C_i$. The crystal size at nucleation is considered as being very small ($r_0 \approx 0$), which leads to negligible modeling errors [3]. In the simulations $\rho_c = 1.296$ g/cm^3, $k_v = 0.24$, and $C_i = 0.0256$ g/g$_{water}$ were used.

The moment ratios μ_1/μ_0, μ_2/μ_0, and μ_3/μ_0 were computed using a high order discretization of the integral (1), both for the model and experiments. These ratios, which are the mean crystal size, area, and volume, normalize out experimental sampling effects that occur as the solids density increases. Ratios of the larger moments are not used due to increased sensitivity to the sampling of large particles [18].

Table 1
Kinetic parameters with 95% confidence intervals for the unseeded crystallization of paracetamol in water, estimated from data collected during the determination of the metastable limit for primary nucleation (k_b is in #/min/g_{water} and k_g is in m/min)

b	$\ln(k_b)$	g	$\ln(k_g)$
6.2 ± 0.9	45.8 ± 4.6	1.5 ± 0.5	-4.1 ± 1.2

The measured solution concentration C and moment ratios μ_1/μ_0, μ_2/μ_0, and μ_3/μ_0 for a series of metastable limit experiments were used to compute maximum likelihood estimates of the four kinetic parameters (k_b, b, k_g, g). The nonlinear optimization was solved using successive quadratic programming. The details of the experimental and parameter estimation procedures are available elsewhere [19]. The resulting kinetic parameters with their confidence intervals are given in Table 1. The results are in very good agreement with growth kinetics reported in the literature [20].

4. Control strategies

The temperature control approach is the simplest and most widely used technique. The only measurement required is the temperature in the crystallizer (and jacket if cascade control is used). Fig. 4 is a schematic diagram of this approach. The controller tracks a setpoint temperature profile in time by manipulating the jacket temperature (via modifying the cooling water flow rate or the ratio between cold and hot water flow rates). The setpoint temperature profile may be obtained using trial-and-error, or open- or closed-loop optimal control if an accurate dynamic model is available. In open-loop optimal control, the setpoint temperature profile is usually parameterised by a linear piecewise function, with the temperatures at the sampling instances being the optimization variables. Various CSD properties have been used as the objective function with the most common being to maximize the mean crystal size

$$L_n = \frac{\mu_1}{\mu_0}. \tag{6}$$

Although the weight-mean crystal size is the most commonly used objective in optimal control studies [3], the weight-mean crystal size is too insensitive to the number of small crystals [5] which can cause significant filtration problems. Using (6), the optimal control problem is:

$$\max_{T(1),T(2),\ldots,T(N)} L_n \tag{7}$$

subject to the constraints of the model Eqs. (2) and

$$T_{\min} \leqslant T(k) \leqslant T_{\max},$$
$$R_{\min} \leqslant \mathrm{d}T/\mathrm{d}t \leqslant R_{\max},$$
$$C_{\text{final}} \leqslant C_{\text{final,max}},$$

where $T_{\min}$, $T_{\max}$,$R_{\min}$, and $R_{\max}$ are the minimum and maximum temperatures and temperature ramp rates, respectively, during the batch. The first two inequality constraints ensure that the temperature profile can be implemented. The last inequality constraint ensures that the minimum yield is achieved as specified by economic considerations. The successive quadratic programming solution of the optimal control problem (7) gives the temperature trajectory in Fig. 5. The initial temperature drop creates nuclei by primary nucleation [21]. The optimum temperature trajectory indicates that, after the seeds are created, the nucleation rate drops off rapidly (see Fig. 6). Note that the growth rate corresponding to the optimum temperature profile is nearly constant after the initial seed generation step of the process, leading to a nearly linear increase in the mean size L_n (see Fig. 5) with the maximum theoretical value at the end of the batch equal to 104 μm, with a yield of 44%.

The optimal temperature trajectory for an unseeded crystallizer first drops the temperature to create seed crystals, followed by an optimal temperature trajectory for a seeded crystallizer. The approach of operating a crystallizer by first operating at high supersaturation to create crystals in situ followed by low supersaturation operation is used in industrial applications of impinging jets and high sheer mixers to crystallization [22–24].

The classical approach requires rather accurate model parameters, or the benefits of optimal control may be lost. Although some uncertainty in the kinetic parameters may be handled through robust feedback control systems [25], there will always be model structure errors (e.g., nonideal mixing) that are not captured by the uncertainty descrip-

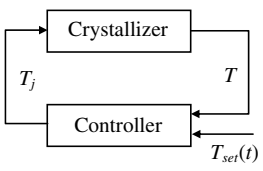

Fig. 4. Schematic block diagram of the classical temperature control approach.

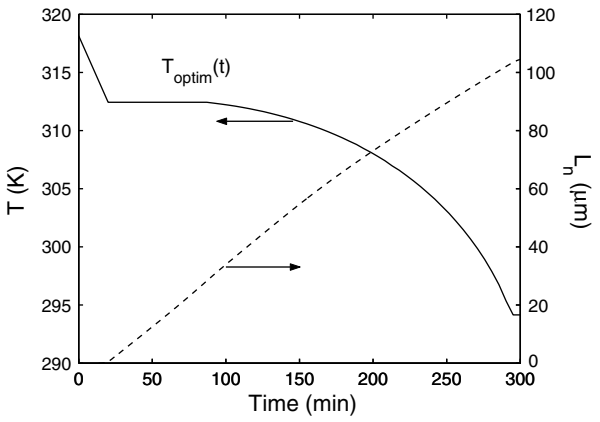

Fig. 5. Simulated optimum temperature profile and change in mean crystal size for the crystallization of paracetamol in water.

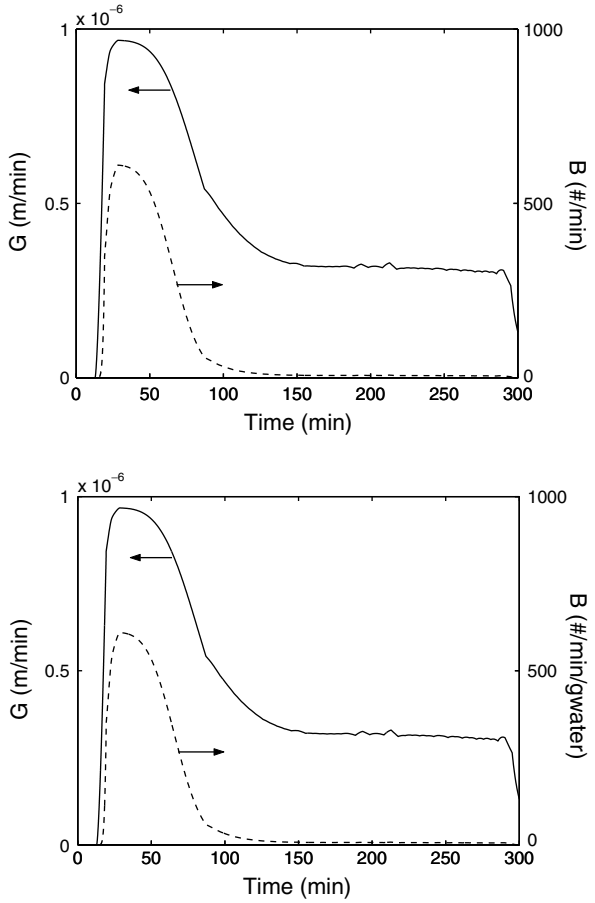

Fig. 6. Variation of the growth rate and nucleation rate corresponding to the optimum temperature profile for the simulated unseeded crystallization of paracetamol in water.

tion. This is partly why the most common method used in industry to design the setpoint temperature profile is by trial-and-error experiments.

The direct design approach shown in Fig. 7 follows a setpoint concentration versus temperature profile within the metastable zone. This approach does not require a detailed model or kinetic parameters. A close-to-optimal concentration versus temperature setpoint can be obtained based on the solubility curve and metastable limit [11,14,26], which can be experimentally determined through automated procedures [11]. Although the close-to-optimal setpoint profile mostly provides very good performance for practical purposes, it is also possible to apply measurement-based optimization approaches [27] to improve the initial setpoint profile according to a run-to-run control scheme, leading to an optimal direct design strategy. This approach could be implemented either by using the initial direct design in the first step and then applying iterative learning control (ILC) to improve the resulted temperature profile, or the C versus T control can be applied repeatedly in the ILC scheme.

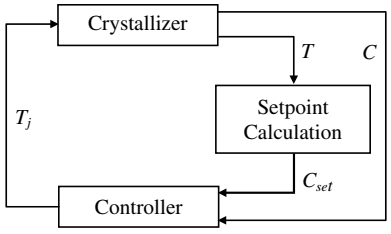

Fig. 7. Schematic block diagram of the concentration versus temperature control approach.

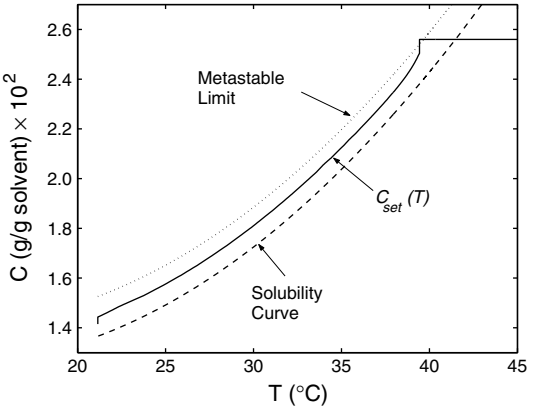

Fig. 8. Setpoint temperature for the concentration-control approach.

Besides the temperature measurement, this approach requires solution concentration measurements, which can be collected using ATR–FTIR spectroscopy, which can produce concentration measurements within 0.1 wt%. The $C_{set}(T)$ trajectory corresponding to the optimum temperature profile from Fig. 5 is shown in Fig. 8. The optimum temperature profile creates a higher supersaturation at the beginning to generate the initial nuclei, then it keeps the supersaturation at a nearly constant value within the metastable zone for the rest of the batch. This is consistent with previous work that indicates that constant supersaturation profiles are close to optimal [9,28,29].

5. Comparing control strategies via simulation

Although the classical T-control and the direct design C-control approaches give identical results under ideal conditions, their sensitivities to disturbances are very different. The effects of uncertainties in the kinetic parameters were evaluated by simulating the two control approaches, using the nonlinear model (2) and considering different error levels in the parameters, with setpoint trajectories computed for the nominal model. The effect of variation in the nucleation exponent on the mean size and the yield is shown in Fig. 9. The mean size at the end of the batch is much more sensitive to variation in the nucleation exponent b for the classical T-control strategy. In addition, the C-control approach leads to constant yield. Unlike T-control where the optimum temperature versus time profile fixes the batch time, in C-control the setpoint is a function of temperature only, leading to variable batch time. Similar trends are obtained for variation in the other kinetic parameters.

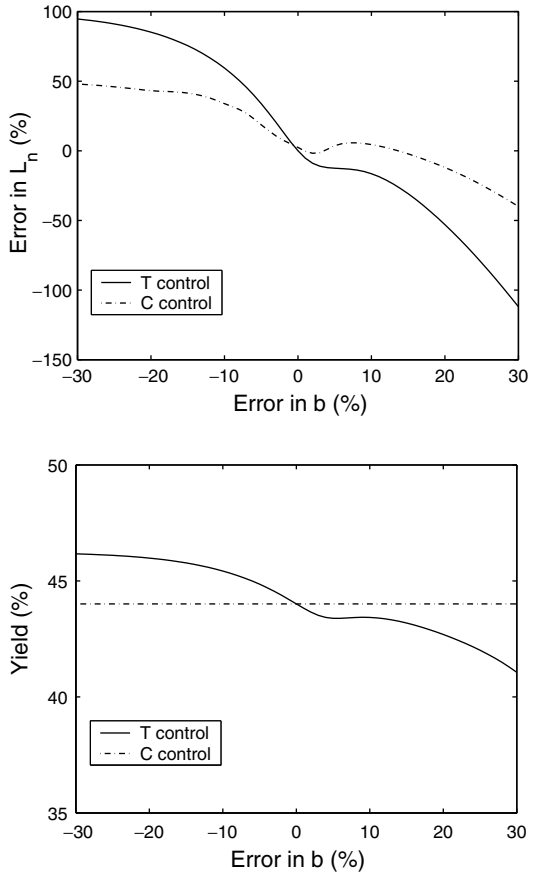

Fig. 9. Sensitivity of the mean crystal size (top) and the crystallizer yield (bottom) to variation in the nucleation exponent b for the two control strategies.

Shifts in the solubility curve typically occur in practice due to the presence of inorganic salts or other contaminants in the feedstocks. Evaporation can also occur. The effects of these disturbances are shown in Table 2. An increase or decrease of 5% in the solubility results in a significant decrease in the mean size. Both control strategies are highly sensitive to shifts in the solubility curve, with T-control being more sensitive. When a linear decrease of the mass of solvent is simulated (e.g., due to evaporation), the C-control approach is much less sensitive than T-control. The concentration measurement in C-control enables the supersaturation to be maintained when solvent is evaporated. The subsequent experimental results confirm and extend the simulation results.

Table 2
Sensitivity of C- and T-control to disturbances

Disturbance		Decrease in mean size L_n (%)	
		T-control	C-control
Shift in solubility curve	−5 %	60	46
	+5 %	61	53
Variation in mass of solvent	−5 %	27	7
	−10 %	49	11

6. Comparing control strategies in practice

Fig. 10 shows the crystals produced by T-control and C-control where the apparatus was designed to operate with as few disturbances as possible. To provide a fair comparison, the setpoint $C_{set}(T)$ profile used in C-control corresponded to the $T_{set}(t)$ trajectory used in T-control (see Fig. 5). Crystals produced under conditions of minimal disturbances exhibited similar shape and size, with slightly less agglomeration for C-control. Even when operating under an artificially low amount of disturbances in the bench-scale experiments, the small disturbances were enough to cause C-control to give a slower average cooling rate, which resulted in the differences in product crystals achieved by the two control strategies. The batch time for T-control was approximately 310 min, whereas for the C-control similar yield was achieved in about 420 min.

The difference in product quality between the two strategies will be much larger at the manufacturing scale, where the disturbances are much more significant. Consider the disturbance where some crystals from a previous batch were not completely removed before starting the next batch. Fig. 11 shows images of the product crystals for T-control and C-control, when some seed was left in the batch. The setpoint trajectory $C_{set}(T)$ was specified to give constant supersaturation after a short period where the temperature dropped to get to the starting point for the setpoint trajectory. The crystals are much larger and uniform in size and shape for C-control than for T-control. C-control gave high crystal product quality even for this rather large disturbance.

This sensitivity of the product quality to a small quantity of seeds for T-control can be understood by inspection

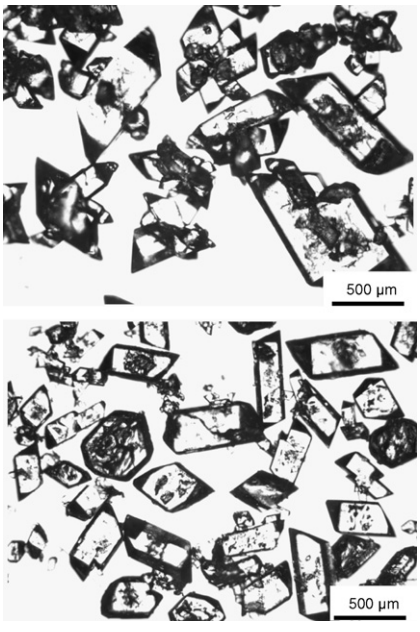

Fig. 10. Microscopy image of paracetamol product crystals for the unseeded system using T-control (top) and C-control (bottom).

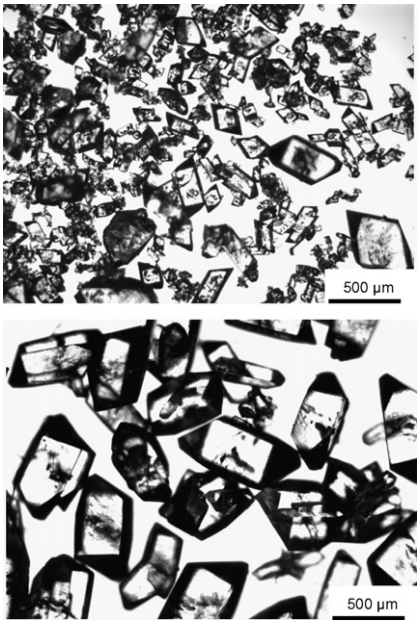

Fig. 11. Microscopy image of paracetamol product crystals for the seeded system using *T*-control with the setpoint obtained from the optimization of the model of the unseeded system (top) and *C*-control (bottom).

of the concentration–temperature diagram in Fig. 12 and the FBRM data in Fig. 13. The same temperature profile was followed for the unseeded and seeded systems to study the effect of the unexpected presence of the small quantity of seed on the performance of *T*-control approach. The temperature setpoint caused the solution concentration to cross the metastable limit initially, as expected, but the presence of seed resulted in lower nucleation at 38 °C than in unseeded operations. This is consistent with nucleation theory, which predicts that the nucleation rate for seeded operations is much lower than for unseeded operations at high supersaturation [9,30]. Hence most of the reduction in supersaturation at 38 °C was due to growth onto the seed crystals rather than the creation of nuclei. The reduced availability of crystal area for growth (less small crystals corresponds to less surface area) caused the supersaturation to drift too far from the solubility curve as the temperature was reduced, crossing the metastable limit and inducing nucleation near the end of the batch run (as indicated by the increased FBRM counts at 5 h). Although a specific crystal–solvent system was selected to illustrate the key points, the physical principles are generally applicable. Temperature control of an unseeded crystallizer will give very poor CSD if some seed is accidentally left behind from a previous batch. In a general sense these experimental results are consistent with the simulation results, which indicated the high sensitivity of *T*-control to variation in the nucleation kinetics.

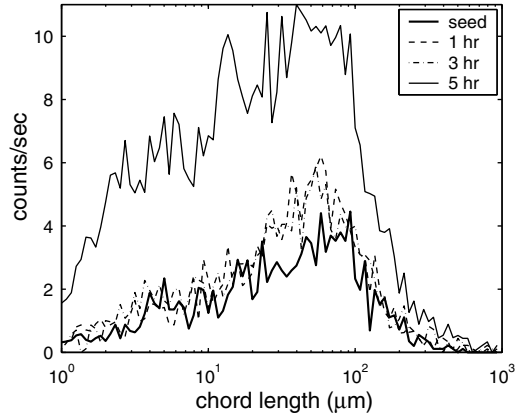

Fig. 13. FBRM chord length distributions at different times during the batch for the *T*-controlled seeded system.

The insensitivity of *C*-control to the seeding can be understood from the concentration–temperature diagram in Fig. 14 and the FBRM data in Fig. 15. The constant value for the supersaturation suppressed nucleation during the batch. Using feedback control to achieve constant supersaturation, without optimizing the setpoint trajectory or seeding, gave much higher quality crystals than the optimized classical *T*-control strategy for this disturbance.

Although the simulation results indicated that *C*-control was less sensitive than the classical *T*-control strategy for

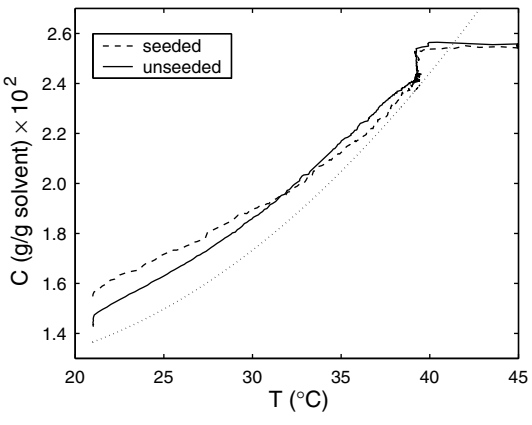

Fig. 12. Concentration–temperature profile of the unseeded and seeded systems operated by *T*-control.

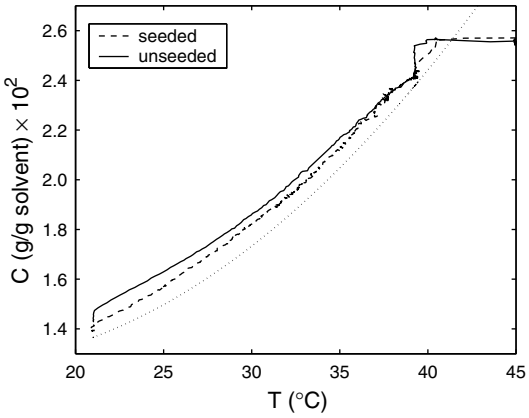

Fig. 14. *C*-control of seeded and unseeded systems. The seeded system was controlled at a lower supersaturation to account for the smaller metastable zone width.

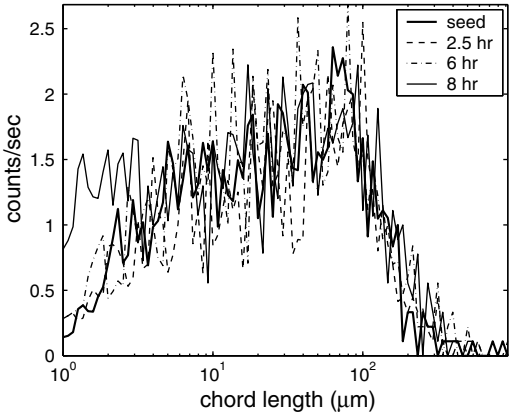

Fig. 15. FBRM chord length distributions at different times during the batch for the *C*-controlled seeded system.

most disturbances, recall that both control strategies are sensitive to a shift in the solubility curve. It is well recognized that the presence of small amount of certain impurities can have substantial effects on the crystallization process. Impurities can cause changes in primary and secondary nucleation kinetics, modify solubility, and/or inhibit or enhance the overall growth rate. Certain impurities have a selective effect on the growth rate of the crystallographic surfaces, thus modifying the crystal shape [9]. The effects of additives on the *C*-control of paracetamol–water crystallization were investigated by introducing 4 mol% acetanilide (AA) to the initial batch. Acetanilide is a structurally related impurity for which moderate primary nucleation inhibition and crystal habit modification effects are reported [31]. AA also has peaks at similar frequencies of the infrared spectra as paracetamol, thus influencing the solution concentration measurements. The *C*-control approach was used to conduct the experiment at the same supersaturation as in the case of the seeded system with *C*-control (with no additive). The FBRM measurements indicated significant nucleation (see Fig. 16) leading to the product shown in Fig. 17 with poor CSD and small

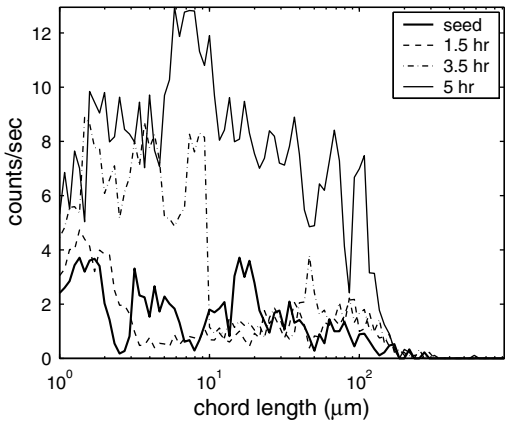

Fig. 16. FBRM chord length distributions at different moments during the batch for the *C*-controlled seeded system with 4 mol% acetanilide additive.

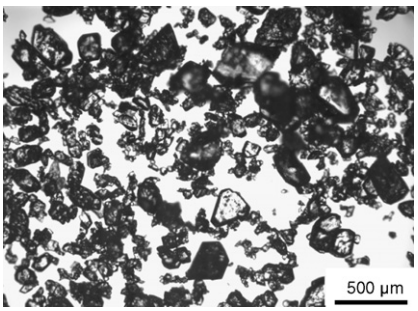

Fig. 17. Microscopy image of paracetamol product crystals for the seeded system using *C*-control and 4 mol% acetanilide as additive.

mean size. This indicates that the effect of additive on the solubility and on the concentration measurement was more significant than its nucleation inhibition effect. These experimental results are in accordance with the simulations, which indicated a significant decrease in the mean size when a shift in solubility occurs. The only way to design control systems to suppress the effects of shifts in the solubility is to include direct measurements of the supersaturation or to include measurements of the particle size distribution directly in the control system.

7. Conclusions

This paper discussed two approaches for the control of batch crystallizers. The temperature control approach is the tradition in batch cooling crystallization. Unless trial-and-error is used to obtain the setpoint profile, an accurate model is required for computing the optimal control trajectory. The direct design approach controls the solution concentration as a function of temperature, so that the desired supersaturation is controlled within the metastable zone. Simulation and experiments indicated that temperature control is highly sensitive to variation in the kinetic parameters and seeding. In contrast, direct design of the concentration-control system requires no information about the model or kinetic parameters of the process, and is instead based on the metastable zone of the system. Concentration-control resulted in lower sensitivity to disturbances than temperature control in almost all cases simulated or tested experimentally. Both control approaches are sensitive to variations in the solubility curve. Also, concentration-control requires a concentration measurement, so the presence of structurally related contaminating chemicals can significantly degrade the performance of this approach.

Acknowledgements

This work was supported by NSF Award #0108053 and the Merck Research Laboratories.

References

[1] R.D. Braatz, Advanced control of crystallization processes, Annu. Rev. Contr. 26 (2002) 87–99.

[2] L.X. Yu, R.A. Lionberger, A.S. Raw, R. D'Costa, H.Q. Wu, A.S. Hussain, Applications of process analytical technology to crystallization processes, Adv. Drug Deliver. Rev. 56 (2004) 349–369.
[3] J.B. Rawlings, S.M. Miller, W.R. Witkowski, Model identification and control of solution crystallization processes: a review, Ind. Eng. Chem. Res. 32 (1993) 1275–1296.
[4] J.W. Eaton, J.B. Rawlings, Feedback control of chemical processes using on-line optimization techniques, Comp. Chem. Eng. 14 (1990) 469–479.
[5] D.L. Ma, R.D. Braatz, Robust identification and control of batch processes, Comp. Chem. Eng. 20 (2003) 1175–1184.
[6] D.L. Ma, S.H. Chung, R.D. Braatz, Worst-case performance analysis of optimal batch control trajectories, AIChE J. 45 (1999) 1469–1476.
[7] B. Srinivasan, D. Bonvin, E. Visser, S. Palanki, Dynamic optimization of batch processes – II. Role of measurements in handling uncertainty, Comp. Chem. Eng. 27 (2003) 27–44.
[8] P. Terwiesc, M. Agarwal, D.W.T. Rippin, Batch unit optimization with imperfect modeling: a survey, J. Process Contr. 4 (1994) 238–258.
[9] J.W. Mullin, Crystallization, third ed., Butterworth-Heinemann, London, 1997.
[10] L.L. Feng, K.A. Berglund, ATR–FTIR for determining optimal cooling curves for batch crystallization of succinic acid, Cryst. Growth Des. 2 (2002) 449–452.
[11] M. Fujiwara, P.S. Chow, D.L. Ma, R.D. Braatz, Paracetamol crystallization using laser backscattering and ATR–FTIR spectroscopy: metastability, agglomeration, and control, Cryst. Growth Des. 2 (2002) 363–370.
[12] H. Grön, A. Borrisova, K.J. Roberts, In-process ATR–FTIR spectroscopy for closed-loop supersaturation control of a batch crystallizer producing monosodium glutamate crystals of defined size, Ind. Eng. Chem. Res. 42 (2003) 198–206.
[13] T. Gutwald, A. Mersmann, Batch cooling crystallization at constant supersaturation. Technique and experimental results, Chem. Eng. Technol. 13 (1990) 229–237.
[14] P. Barrett, B. Glennon, Characterizing the metastable zone and solubility curve using Lasentec FBRM and PVM, Chem. Eng. Res. Des. 80 (2002) 799–805.
[15] T. Togkalidou, M. Fujiwara, S. Patel, R.D. Braatz, Solute concentration prediction using chemometrics and ATR–FTIR spectroscopy, J. Cryst. Growth 231 (2001) 534–543.
[16] E.J. Hukkanen, R.D. Braatz, Measurement of particle size distribution in suspension polymerization using in situ laser backscattering, Sensor. Actuator. B 96 (2003) 451–459.
[17] S.M. Miller, J.B. Rawlings, Model identification and control strategies for batch cooling crystallizers, AIChE J. 40 (1994) 1312–1327.
[18] R. Gunawan, D.L. Ma, M. Fujiwara, R.D. Braatz, Identification of kinetic parameters in a multidimensional crystallization process, Int. J. Mod. Phys. B 16 (2002) 367–374.
[19] Z.K. Nagy, M. Fujiwara, R.D. Braatz, Determination of kinetic parameters for batch pharmaceutical crystallization using metastable zone experiments, University of Illinois at Urbana-Champaign, Technical Report, 2002.
[20] R.A. Granberg, D.G. Bloch, A.C. Rasmuson, Crystallization of paracetamol in acetone–water mixtures, J. Cryst. Growth 198/199 (1999) 1287–1293.
[21] N. Doki, N. Kubota, M. Yokota, S. Kimura, S. Sasaki, Production of sodium chloride crystals of uni-modal size distribution by batch dilution crystallization, J. Chem. Eng. Jpn 35 (2002) 1099–1104.
[22] M. Midler Jr., E.L. Paul, E.F. Whittington, M. Futran, P.D. Liu, J. Hsu, S.-H. Pan, Crystallization method to improve crystal structure and size, US Patent No. 5,314,506 (1994).
[23] J.M. Hacherl, E.L. Paul, H.M. Buettner, Investigation of impinging jet crystallization with a calcium oxalate model system, AIChE J. 49 (2003) 2352–2362.
[24] J. Werling, J.E. Kipp, R. Sriram, M.J. Doty, Method for preparing submicron suspensions with polymorph control, US Patent No. 6,977,085 (2005).
[25] Z.K. Nagy, R.D. Braatz, Open- and closed-loop robust optimal control of batch processes using distributional worst-case analysis, J. Process Contr. 14 (2004) 411–422.
[26] F. Lewiner, G. Fevotte, J.P. Klein, F. Puel, Improving batch cooling seeded crystallization of an organic weed-killer using on-line ATR–FTIR measurement of supersaturation, J. Cryst. Growth 226 (2001) 348–362.
[27] C. Welz, B. Srinivasan, D. Bonvin, Combined on-line and run-to-run optimization of batch processes with terminal constraints, in: Proceedings of the IFAC Symposium on Advanced Control of Chemical Processes, Elsevier Scientific, Oxford, UK, 2004, pp. 55–62.
[28] J.W. Mullin, .J. Nývlt, Programmed cooling of batch crystallizers, Chem. Eng. Sci. 26 (1971) 369–377.
[29] A.G. Jones, J.W. Mullin, Programmed cooling crystallization of potassium sulphate solutions, Chem. Eng. Sci. 29 (1974) 105–118.
[30] K.-J. Kim, A. Mersmann, Estimation of metastable zone width in different nucleation processes, Chem. Eng. Sci. 56 (2001) 2315–2324.
[31] B.A. Hendriksen, D.J.W. Grant, P. Meenan, D.A. Green, Crystallization of paracetamol (acetaminophen) in the presence of structurally related substances, J. Cryst. Growth 183 (1998) 629–640.